

A-Si:H/C-Si Heterointerface Formation And Epitaxial Growth Studied By Real-Time Optical Probes

Nirbhay Singh Parmar

Department of Mechanical Engineering

IIMT University, Meerut, India

nirbhaysparmar@gmail.com

Abstract: we have observed formation of both a-Si:H and epi-Si films with SE, ATR-FTIR, and SHG. The three combined techniques provide a method to distinguish between direct heterointerface formation and nanometer-level epitaxial growth and yield therefore means to investigate and control processes occurring during Si thin film growth on H terminated Si, both nonintrusively and in real time.

I. INTRODUCTION

Ultrathin silicon films deposited on H terminated crystalline silicon (c-Si) substrates are of significant importance in photovoltaics, either as hydrogenated amorphous silicon (a-Si:H) films for surface passivation¹² and silicon heterojunction (SHJ) formation³ or as epitaxial silicon (epi-Si) films for solar cell concepts based on thin film c-Si technology.^{4,5} The performance of these devices is highly governed by their interface quality. For high- performance SHJ solar cells it is essential to form an abrupt and atomically flat a-Si:H/c-Si interface with any nanometer-level epi-Si formation being detrimental.^{6,7} For Si epitaxy, a layer of perfectly crystalline Si is desired suppressing defect incorporation and polycrystalline or amorphous Si formation.⁵ The film morphology is influenced by several factors, such as the deposition temperature, the substrate surface nature, as well as the growth rate, surface roughness, and H content of the developing film.^{4,7-9} However, the underlying mechanistic factors controlling whether a film develops entirely epitaxial or purely amorphous with a sharp interface are not fully understood yet and, evidently, more insight into the initial Si film formation is required.

Most previous studies in this field have been carried out using elaborate ex situ techniques such as transmission electron microscopy (TEM).^{4,6} More recently, in situ optical techniques capable of monitoring film properties during deposition have been applied such as spectroscopic ellipsometry (SE) and attenuated total internal reflection Fourier transform infrared spectroscopy (ATR-FTIR) to probe the films' linear optical properties and H bonding, respectively.^{3,5,7,8,10,11} In this letter, we apply SE and ATR-FTIR simultaneously with the nonlinear optical technique of second-harmonic generation (SHG) to study the evolution of Si film morphology during deposition on c-Si. Being surface and interface specific and sensitive to Si-Si bonds, SHG allows for direct probing of the properties of the interface between Si films and the c-Si substrate.¹²⁻¹⁴ Films have been deposited at a temperature of 150 °C, i.e., within the typical transition region from amorphous to epitaxial film growth,^{7,8} yielding different film morphologies.

It is demonstrated that the three optical probes provide insight into heterointerface formation and epitaxial growth, at a level unprecedented by nonintrusive and real-time probes.

The Si thin films were deposited using hot-wire chemical vapor deposition in a setup with a base pressure of $< 10^{-9}$ mbar. A 0.45-mm-diameter tungsten filament was resistively heated to about 2000 °C to dissociate SiH_4 gas at a pressure of 8×10^{-3} mbar. The substrates were either standard P-doped Si(100) wafers (resistivity of 10-30 Ω cm) or undoped trapezoidally shaped Si(100) substrates for experiments involving ATR-FTIR (25 reflections at working surface). Two different sample cleaning and processing conditions were applied: an ultrasound ethanol bath and subsequent immersion in a 2% HF solution for 2 min (treatment A) or a standard RCA I and RCA II procedures using a buffered 1% $\text{NH}_4\text{F}/\text{HF}$ solution

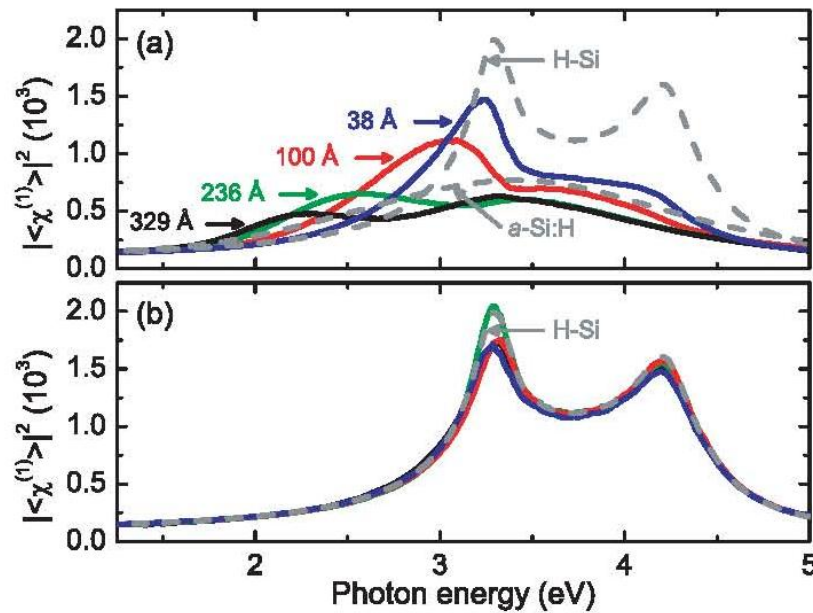


FIG. 1 Squared pseudolinear susceptibility $|X^{(1)}|^2$ obtained with SE during deposition for (a) a-Si:H films and for (b) epi-Si films on Si(100). For both (a) and (b) data are given for film thicknesses of 38, 100, 236, and 329 Å. Dashed lines indicate $|X^{(1)}|^2$ of a H-Si(100) substrate and $X^{(1)}|^2$ of a-Si:H as deduced from the data.

(BHF) with pH 4 (treatment B). Both methods removed the native oxide terminating the Si surface with H. Directly after cleaning, the samples were mounted into the setup. Prior to deposition on the HF cleaned samples (A), the setup was baked for 16 h with the samples reaching a temperature of 225 °C. The deposition on the BHF cleaned samples (B) was started once reaching a temperature of 150 °C and a background pressure of 10^{-7} mbar, typically < 60 min after loading. The filament was placed at 11 cm from the HF cleaned samples (A) and at 13 cm from the BHF cleaned samples (B), resulting in deposition rates of 3.4 and 2.1 nm/min, respectively. The optical schemes for the SE, ATR-FTIR, and SHG measurements are described in detail elsewhere.^{11,14} Briefly, the vacuum system was equipped with a rotating compensator ellipsometer and Fourier transform interferometer for the SE and ATR-FTIR measurements, respectively, whereas a tunable Ti:sapphire oscillator provided the femtosecond laser radiation for the SHG measurements. The time resolutions for SE, ATR-FTIR, and SHG were 3.5, 6.8, and 0.1 s, respectively. SE results will be expressed in terms of the squared pseudolinear susceptibility, $|X^{(1)}|^2 = |(\epsilon_1 - 1)|^2 + (\epsilon_1)^2$, which

is calculated from the raw SE data by treating the film and substrate as one semi-infinite material. This representation facilitates the comparison with the SHG intensity that is proportional to the squared second-order nonlinear susceptibility $|(X^{(2)})|^2$.

Figure 1 shows the squared pseudolinear susceptibility $|(X^{(1)})|^2$ measured with SE during Si film deposition, whereas also $|(X^{(1)})|^2$ of the *H-Si(100)* substrate at 1 50 °C and the linear susceptibility $|(X^{(1)})|^2$ of a-Si:H deduced from the SE data are shown. The spectra in Fig. 1(a), obtained after

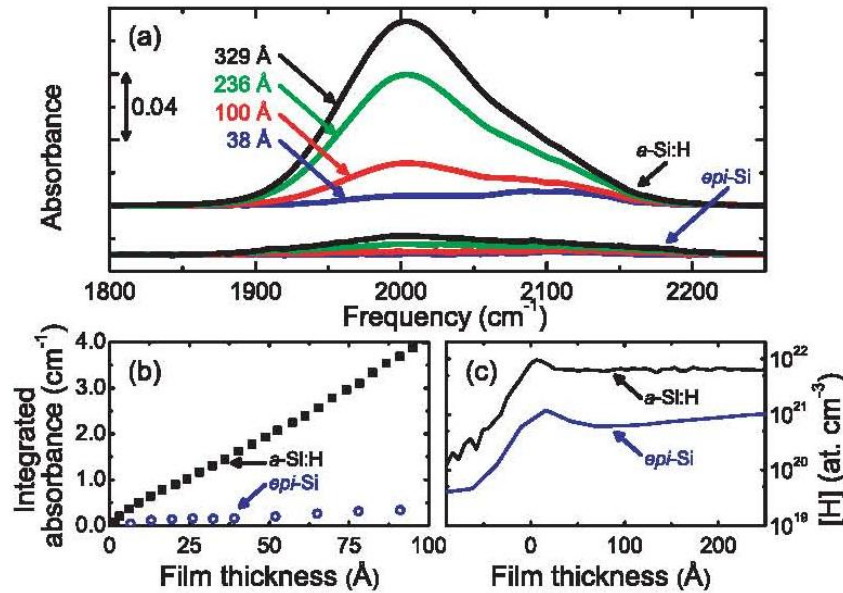


FIG. 2 (a) ATR-FTIR spectra for an a-Si:H and a predominantly epitaxial film at a thickness of 38, 100, 236 and 329 Å obtained during deposition on Si(100). **(b)** Integrated absorbance for a-Si:H and predominantly epi-Si as a function of film thickness. **(c)** H content obtained from TOF-SIMS analysis for the same films.

treatment A, clearly indicate the deposition of a-Si:H; with increasing film thickness the E'_0/E_1 and E_2 critical point resonances broaden and ultimately cannot be separately distinguished anymore. The spectra in Fig. 1(b), obtained after treatment B, correspond to films with the same thickness as in Fig. 1(a). The spectra hardly change with increasing film thickness revealing that the films developed epitaxially. Comparison with optical modeling indicates that the surface roughness does not significantly change with film thickness and is comparable to the substrate roughness. This is corroborated by atomic force microscopy yielding an unchanged rms roughness of ~ 3 Å. At around 3.3 eV an oscillation in $|(X^{(1)})|^2$ is observed as a function of film thickness in Fig. 1(b). Teplin et al. attributed this behavior to interference due to a porous interface layer.⁵ The SE results clearly show that substrate treatment has a great influence on film morphology.

ATR-FTIR spectra in Fig. 2(a) show the formation of an a-Si:H film after treatment A and a film with a high fraction of epi-Si after treatment B. In Fig. 2(b) the integrated absorbance deduced from the spectra is shown. Obviously, the absorbance of the a-Si:H is about an order of magnitude higher than for the predominantly epitaxial material and consequently the amount of H incorporated in the a-Si:H film is much higher. The maxima of the spectra shift to lower wave numbers with increasing a-Si:H and epi-Si thickness and the integrated absorbance

increases more rapidly during initial growth, similar as reported for a-Si:H in Ref. 3. Both phenomena indicate a H-rich onset of film growth, which causes a poorer initial network structure.³¹¹ After ~ 40 Å of a-Si:H deposition the integrated absorbance increases linearly as a function of

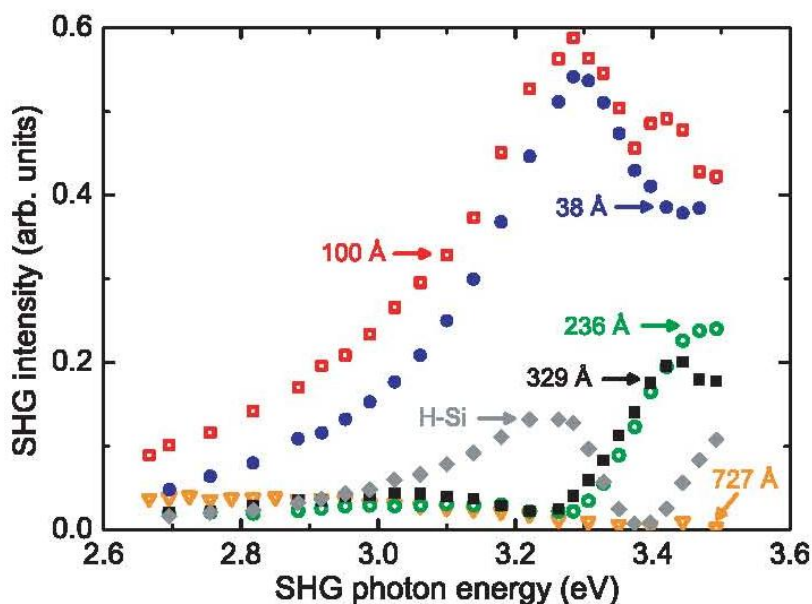


FIG. 3 SHG spectra for p polarized fundamental and SHG radiation for a-Si:H films deposited on Si(100) and for a pristine H-Si(100) surface at 150 °C.

film thickness indicating a constant H incorporation during bulk film growth. These results are corroborated by time-of-flight secondary ion mass spectrometry (TOF-SIMS) analysis of both films [Fig. 2(c)], featuring also the H-rich interface between the substrate and film. The H content in the epi-Si film is about an order of magnitude lower and increases during bulk growth, indicating a gradual increase of the amorphous fraction. The evolution of the H content, in addition to surface roughness, has been suggested to play an important role in the breakdown process of epi-Si.⁹

SHG spectra obtained at 150 °C right after deposition of a-Si:H films with different thicknesses are shown in Fig. 3, all after treatment A. The spectrum of the pristine H-Si(100) starting surface (also shown) exhibits the same characteristic behavior with a sharp minimum at 3.40 eV as reported by Dadap et al.¹² indicating a good H termination of the surface. For ultrathin a-Si:H films of 38 and 100 Å the SHG intensity is enhanced and has a sharp resonance at 3.3 eV and an additional possibly broader contribution, best visible above 3.4 eV. For the 236 and 329 Å films the intensity is reduced again and shows a minimum around 3.25 eV. For a thick film of 727 Å the SHG intensity is very low, particularly in the high photon energy range. As the SHG radiation, especially for high photon energies, is absorbed while propagating through the a-Si:H film, the decreasing SHG intensity for thicker films suggests (similar to Ref. 14) that the SHG radiation is predominantly generated at the a-Si:H/c-Si interface. For very thin a-Si:H films the SHG spectrum has a similar shape as the linear susceptibility for c-Si, which also has a sharp resonance at 3.3 eV (cf. Fig. 1). This similarity indicates that these SHG spectra are dominated by interband transitions related to Si-Si bonds in the c-Si at the interface. The second, possibly broader, contribution to SHG originates most likely from Si-Si bonds of a-Si:H.^{13,14}

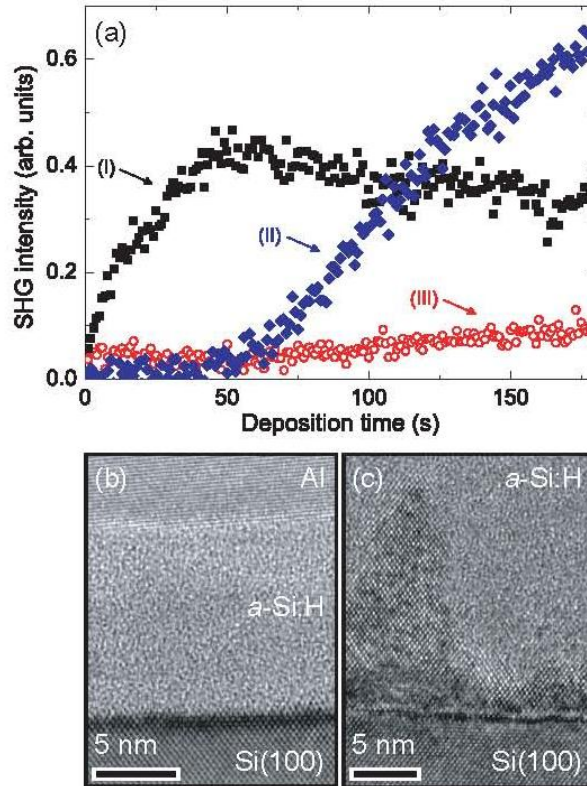


FIG. 4 (a) SHG intensity as a function of deposition time at a SHG photon energy of 3.40 eV for p polarized fundamental and SHG radiation for (I) an a-Si:H film, (II) an a-Si:H film with epitaxial onset of growth (~ 20 Å), and (III) a fully epi-Si film. (b) Cross sectional TEM image of film I. (c) Cross sectional TEM image of film II.

The SHG spectra demonstrate the sensitivity of SHG to the interface between c-Si and a-Si:H, indicating that real-time SHG can provide insight into interface formation. In Fig. 4(a) the SHG intensity as a function of deposition time is shown for films (I and II) formed after treatment A and for a film (III) formed after treatment B. The SHG photon energy was 3.40 eV, which is close to the E_0'/E critical point of c-Si and corresponds to the minimum in the SHG spectrum for H-Si(100) at the deposition temperature of 150°C. The SHG intensity of film I increases rapidly at the onset of deposition, while the intensity for film II increases after a period of ~ 50 s, corresponding to ~ 20 Å of film growth. For increasing film thickness the SHG intensity decreases again (not shown), in agreement with the SHG spectra in Fig. 3. The SHG intensity for film III shows only a very slight increase with increasing film thickness. Realtime SE and ATR-FTIR experiments indicate that films I and II are both amorphous, while the real-time SHG response of both films in Fig. 4(a) is significantly different. Cross sectional high resolution TEM images, shown in Figs. 4(b) and 4(c), reveal that film I developed fully amorphous, whereas the onset of growth for film II was epitaxial, followed by rapid breakdown into mixed phase material after ~ 20 Å, and finally formation of purely amorphous material. Film III developed fully epitaxial (not shown). It can be concluded that the difference in initial film growth strongly influences the real-time behavior of the SHG intensity. Epi-Si growth hardly modifies the real-time SHG intensity, whereas the intensity increases rapidly once amorphous film growth commences.

The two sample treatments clearly influenced the structure of the films deposited. To quantify the surface quality of the substrates the imaginary part of the pseudodielectric function (ϵ_2) at the E_2 critical point energy as measured with SE can be used.¹⁵ Treatment A (B) resulted in (ϵ_2) = 39.0 ± 0.9 (39.5 ± 0.9) at room temperature directly after cleaning and 38.1 ± 0.9 (38.6 ± 1.1) at 150 °C just prior to deposition. Consequently, treatment B yields a slightly higher quality surface compared to A without a noticeable degradation by the baking of the substrate in A. The different morphology of the films formed after the two procedures might therefore be related to surface roughness: for Si(100) both treatments create a relatively rough surface; however, for treatment B the surface roughness is more ordered with (111) facets.¹⁶ Also the SHG spectra of the pristine H-Si(100) indicate differences in substrate surface properties after the two treatments. The slightly lower growth rate after treatment B might also be beneficial for epitaxial growth; however, the influence is expected to be subordinate to that of the substrate properties.

II. CONCLUSION

,we have observed formation of both a-Si:H and epi-Si films with SE, ATR-FTIR, and SHG. The three combined techniques provide a method to distinguish between direct heterointerface formation and nanometer-level epitaxial growth and yield therefore means to investigate and control processes occurring during Si thin film growth on H terminated Si, both nonintrusively and in real time.

ACKNOWLEDGEMENT

This work was supported by the Netherlands Foundation for Fundamental Research on Matter (FOM). The research of one of the authors (W.M.M.K.) has been made possible by a fellowship of the Royal Netherlands Academy of Arts and Sciences (KNAW).

REFERENCES

- [1] S. de Wolf and G. Beaucarne, Appl. Phys. Lett. 88, 022104 (2006).
- [2] S. de Wolf and M. Kondo, Appl. Phys. Lett. 90, 0421 1 1 (2007).
- [3] H. Fujiwara and M. Kondo, Appl. Phys. Lett. 86, 0321 1 2 (2005).
- [4] D.J. Eaglesham, H.-J. Gossmann, and M. Cerullo, Phys. Rev. Lett. 65, 1227 (1990).
- [5] C.W. Teplin, D.H. Levi, E. Iwaniczko, K.M. Jones, J.D. Perkins, and H.M. Branz, J. Appl. Phys. 97, 103536 (2005).
- [6] Y. Yan, M. Page, T.H. Wang, M.M. Al-Jassim, H.M. Branz, and Q. Wang, Appl. Phys. Lett. 88, 121925 (2006).
- [7] H. Fujiwara and M. Kondo, Appl. Phys. Lett. 90, 013503 (2007).
- [8] D.H. Levi, C.W. Teplin, E. Iwaniczko, T.H. Wang, and H.M. Branz, J. Vac. Sci. Technol A 24, 1676 (2006).
- [9] J. Thiesen, H.M. Branz, and R.S. Crandall, Appl. Phys. Lett. 77, 3589 (2000).
- [10] Y.M. Li, I. An, H.V. Nguyen, C.R. Wronski, and R.W. Collins, Phys. Rev. Lett. 68, 2814 (1992).
- [11] P.J. van den Oever, J.J.H. Gielis, M.C.M. van de Sanden, and W.M.M. Kessels, Thin Solid Films, 516, 51 1 (2008).

- [12] J.I. Dadap, Z. Xu, X.F. Hu, M.C. Downer, N.M. Russell, J.G. Ekerdt, and O.A. Aktsipetrov, *Phys. Rev. B* 56, 13367 (1997).
- [13] I.M.P. Aarts, J.J.H. Gielis, M.C.M. van de Sanden, and W.M.M. Kessels, *Phys. Rev. B* 73, 045327 (2006).
- [14] J.J.H. Gielis, P.M. Gevers, A.A.E. Stevens, H.C.W. Beijerinck, M.C.M. van de Sanden, and W.M.M. Kessels, *Phys. Rev. B* 74, 16531 1 (2006); Chapter 3 of this thesis.
- [15] T. Yasuda and D.E. Aspnes, *Appl. Opt.* 33, 7435 (1994).
- [16] P. Dumas, Y.J. Chabal, and P. Jakob, *Surf. Sci.* 269/270, 867 (1992).